

Study of Electron-Vibrational Interaction in Molecular Aggregates Using Mean-Field Theory: From Exciton Absorption and Luminescence to Exciton-Polariton Dispersion in Nanofibers.

Boris D. Fainberg*

Faculty of Sciences, Holon Institute of Technology, 52 Golomb St., Holon 58102, Israel
Tel Aviv University, School of Chemistry, Tel Aviv 69978, Israel

Abstract

We have developed a model in order to account for electron-vibrational effects on absorption, luminescence of molecular aggregates and exciton-polaritons in nanofibers. The model generalizes the mean-field electron-vibrational theory developed by us earlier to the systems with spatial symmetry, exciton luminescence and the exciton-polaritons with spatial dispersion. The correspondence between manifestation of electron-vibrational interaction in monomers, molecular aggregates and exciton-polariton dispersion in nanofibers is obtained by introducing the aggregate line-shape functions in terms of the monomer line-shape functions. With the same description of material parameters we have calculated both the absorption and luminescence of molecular aggregates and the exciton-polariton dispersion in nanofibers. We apply the theory to experiment on fraction of a millimeter propagation of Frenkel exciton polaritons in photoexcited organic nanofibers made of thiocyanine dye.

1 Introduction

The emission of light by Frenkel excitons in organic excitonic materials, e.g. dye molecules, polymers and biological structures including bioinspired peptide beta sheet nanostructures, is used in many photonic applications, including wave guiding, lasers etc.^{1–15} Frenkel excitons are formed by the Coulomb

interaction between molecules, so that in the majority of cases photoemission from excitons is accompanied by the exciton annihilation and the photon creation where two (quasi-) particles (exciton and photon) can be considered separately. In contrast, in ordered materials with large oscillator strength possessing strong absorption, excitons that determine the medium polarization and photons (transverse field) are strongly coupled forming new elementary excitations: polaritons.^{10,11,16,17} Exciton polaritons (EPs) possess properties of both light and matter. Cavity EPs have a mass thanks to their excitonic part that enables us to consider them as an interacting Bose gas¹⁸ leading to Bose-Einstein condensation.¹⁹ The latter results in macroscopic coherence of the condensate and superfluidity.²⁰ In addition, polariton condensation enables us to realize low threshold polariton lasing without population inversion achieved with conventional nanosecond excitation.⁹ Recently topological insulators in EP systems organized as a lattice of coupled semiconductor microcavities in magnetic field were suggested^{21,22} and implemented.²³

Furthermore, electron-vibrational interactions in molecular systems have a pronounced effect on EPs resulting among other things in decay and their instability. One way of taking the decay into account is the introduction of complex frequencies with the imaginary part describing phenomenologically constant damping rates (Markovian relaxation).^{24,25} In general, taking the effect of strong electron-

vibrational interactions on the EPs into account is a non-trivial problem. The point is that in this case both the interaction with radiation field and electron-vibrational interaction should be considered as strong.²⁶ La Rocca *et al.*^{25,27} studied polariton dispersion in organic-based microcavities taking a single high-frequency (HF) optically active (OA) intramolecular vibration into account introducing also complex exciton replicas frequencies (see above).

However, in real situations the relaxation of molecular and excitonic systems is non-Markovian and cannot be described using constant decay rates resulting in the Lorentzian shape of spectra. Using such a description, one may simulate a separate spectrum of an exciton⁶ or even polaritonic luminescence³ using fitting parameters, but cannot describe the transformation of spectra when for example monomers form an aggregate etc.²⁸ (see also²⁹). The matter is that if the monomer spectrum has Lorentzian shape, the aggregate spectrum is simply shifted monomer spectrum.²⁸ At the same time, other shapes that non-Markovian theory leads to are able to describe the transformation of spectra including strong narrowing the J-aggregate absorption spectrum with respect to that of a monomer.²⁸

It is worth noting that actual dissipative properties of the vibrational system are very important for EPs, in particular, for EP fluorescence propagating in organic nanofibers.³ The point is that a "blue" part of the fluorescence spectrum overlaps with the wing of the imaginary part of the wave number defining absorption and, therefore, is partly absorbed.^{3,28}

In Ref.²⁸ we developed a mean-field electron-vibrational theory of Frenkel EPs in organic dye structures and applied it to the aggregate absorption and the experiment on long-range polariton propagation in organic dye nanofibers at room temperature.^{3,4} The theory is non-Markovian and is able to describe the transformation of absorption spectra on molecular aggregation. In the present work we generalize the theory developed in Ref.²⁸ to the systems with spatial symmetry (like organic molecular crystals), to the exciton luminescence and the exciton-polaritons with spatial dispersion. The matter is that ordered structures include among other things also organic dye nanofibers^{1,3} that are synthesized

by self-assembly of thiacyanine (TC) dye molecules in solution. We obtain the correspondence between manifestation of electron-vibrational interaction in monomers, molecular aggregates and exciton-polaritons in nanofibers. With the same description of material parameters we calculate both the absorption and luminescence of molecular aggregates and the exciton-polariton dispersion in nanofibers. We apply the theory to experiment on fraction of a millimeter propagation of Frenkel exciton polaritons in photoexcited organic nanofibers made of TC dye.^{3,4}

The paper is organized as follows. We start with the derivation of the mean-field equations in ordered structures taking electron-vibrational and dipole-dipole intermolecular interactions in condensed matter into account. Then we solve these equation in the momentum representation, Section 2.1. In Section 3 we calculate polarization, susceptibility and dielectric function in the \mathbf{k} space. In Section 4 we calculate the relaxed luminescence of aggregates for weak excitation. The exciton luminescence and absorption spectra in our mean-field theory obey Stepanov's law.^{11,30} Our theory describes both narrowing the J-aggregate absorption and luminescence spectra, and diminishing the Stokes shift between them with respect to that of a monomer. In Section 5 we apply the theory to experiment on fraction of a millimeter propagation of EPs in photoexcited fiber-shaped H-aggregates of TC dye at room temperature³ bearing in mind the correspondence between manifestation of electron-vibrational interaction in monomers, molecular aggregates and EP dispersion in nanofibers, and in Section 6, we briefly conclude.

2 Derivation of Equations for Expectation Value of Excitonic Operator in Ordered Structures

In this section we shall consider an ensemble of molecules with two electronic states $n = 1$ (ground) and 2 (excited) in a condensed matter described by

the exciton Hamiltonian

$$H_{exc} = H_0 + H_{int} \quad (1)$$

Here the molecular Hamiltonian, H_0 , is given by

$$H_0 = \sum_{j=1}^2 [E_j + W_j(\mathbf{Q})] \sum_m |mj\rangle \langle mj| \quad (2)$$

where $E_2 > E_1$, E_j is the energy of state j , $W_j(\mathbf{Q})$ is the adiabatic Hamiltonian of the vibrational subsystem of a molecule interacting with the two-level electron system under consideration in state j . The dipole-dipole intermolecular interactions in the condensed matter are described by the interaction Hamiltonian^{31,32}

$$H_{int} = \hbar \sum_m \sum_{n \neq m} J_{mn} b_m^\dagger b_n \quad (3)$$

where J_{mn} is the resonant exciton coupling, $b_m = |m1\rangle \langle m2|$ is the operator that describes the annihilation of an excitation in molecule m at level 2, and $b_m^\dagger = |m2\rangle \langle m1|$ is the operator that describes the creation of an excitation of molecule m to level 2. We adopt here the Coulomb cause for the electromagnetic field, according to which the Coulomb interaction between molecules is conditioned by the virtual scalar and longitudinal photons.^{11,31} In addition, the interaction conditioned by the transverse photons exists, quantum electromagnetic field $\hat{\mathbf{E}}(t)$,

$$\hat{\mathbf{E}}(\mathbf{r}, t) = \frac{1}{2} \left\{ \sum_{\mathbf{q}} \mathbf{e}_{\mathbf{q}} \mathcal{E}_{\mathbf{q}} \exp[i(\mathbf{q} \cdot \mathbf{r} - \omega_{\mathbf{q}} t)] + \text{h.c.} \right\}, \quad (4)$$

Then the system Hamiltonian takes the form

$$H = H_{exc} + \hbar \sum_{\mathbf{q}} \omega_{\mathbf{q}} a_{\mathbf{q}}^\dagger a_{\mathbf{q}} - \hat{\mathbf{D}} \cdot \hat{\mathbf{E}} \quad (5)$$

Here $\mathbf{e}_{\mathbf{q}} \mathcal{E}_{\mathbf{q}} \exp(i\mathbf{q} \cdot \mathbf{r}) = i2\sqrt{2\pi\hbar\omega_{\mathbf{q}}} a_{\mathbf{q}} u_{\mathbf{q}}(\mathbf{r})$ is the field amplitude, $a_{\mathbf{q}}$ is the annihilation operator for mode \mathbf{q} , $\mathbf{e}_{\mathbf{q}}$ is the unit photon polarization vector, V is the photon quantization volume, $u_{\mathbf{q}}(\mathbf{r})$ describes a space dependence of the field amplitude where $u_{\mathbf{q}}(\mathbf{r}) = \mathbf{e}_{\mathbf{q}} \exp(i\mathbf{q} \cdot \mathbf{r}) V^{-1/2}$ for plane waves, and $\hat{\mathbf{D}}$

is the dipole moment operator of a molecule. The latter can be written as $\hat{\mathbf{D}} = \mathbf{D} \sum_m (b_m + b_m^\dagger)$ with \mathbf{D} the electronic transition dipole moment. It is worth noting that if one wants to introduce photons in a cavity, he uses the cavity eigenmodes for the expansion instead of plane waves.

Among other things the interaction, the term " $-\hat{\mathbf{D}} \cdot \hat{\mathbf{E}}$ " is responsible for the creation of EPs. In an experiment related to a linear absorption by excitons one can consider the electromagnetic field classically. In that case one can use the same formula (4) considering $\mathbf{E}(\mathbf{r}, t)$ and $\mathcal{E}_{\mathbf{q}}$ as classical function. In this work we also consider a luminescence experiment where the electromagnetic field may be decomposed into two modes: classical (incoming field), and quantum (the scattered field mode generated by spontaneous emission), Eq.(4). In any case, the field frequency, $\omega_{\mathbf{q}}$, is close to that of the transition $1 \rightarrow 2$.

Consider structures that are symmetric in space like organic molecular crystals. Such structures include also organic dye nanofibers^{1,3} that are synthesized by self-assembly of TC dye molecules in solution.

We define the exciton annihilation $b_{\mathbf{k}}$ and creation $b_{\mathbf{k}}^\dagger$ operators in the momentum representation^{11,31}

$$b_{\mathbf{k}} = \frac{1}{\sqrt{\mathcal{N}}} \sum_m b_m \exp(-i\mathbf{k} \cdot \mathbf{r}_m) \quad (6)$$

$$b_{\mathbf{k}}^\dagger = \frac{1}{\sqrt{\mathcal{N}}} \sum_m b_m^\dagger \exp(i\mathbf{k} \cdot \mathbf{r}_m) \quad (7)$$

and the lattice Fourier transform of intermolecular interaction^{10,11,17}

$$J(\mathbf{k}) = \sum_{n \neq m} J_{mn} \exp[i\mathbf{k} \cdot (\mathbf{r}_n - \mathbf{r}_m)] \quad (8)$$

where \mathcal{N} is the number of interacting molecules. Then

$$b_n = \frac{1}{\sqrt{\mathcal{N}}} \sum_{\mathbf{k}} b_{\mathbf{k}} \exp(i\mathbf{k} \cdot \mathbf{r}_n) \quad (9)$$

It should be noted that $J(0) = \sum_{n \neq m} J_{mn} = -p$ where p is the parameter of intermolecular interaction used in Ref.²⁸

In the absence of vibrations, the unitary transformation, Eqs. (6), (7), (8) and (9), enables us to diagonalize the electronic part of the excitonic Hamiltonian, H_{exc} , considering $b_{\mathbf{k}}$ as Bose operators

$$b_{\mathbf{k}'}b_{\mathbf{k}}^\dagger - b_{\mathbf{k}}^\dagger b_{\mathbf{k}'} = \delta_{\mathbf{k}\mathbf{k}'} \quad (10)$$

that is correct for weak excitation. In that case using the Heisenberg equations of motion, one obtains that \hat{H}_{int} gives the following contribution to the change of the excitonic operator $b_{\mathbf{k}}$ in time

$$\frac{d}{dt}b_{\mathbf{k}} \sim \frac{i}{\hbar}[\hat{H}_{int}, b_{\mathbf{k}}] = -iJ(\mathbf{k})b_{\mathbf{k}} \quad (11)$$

Now let us take the vibrational subsystem of molecules into account. Since an absorption spectrum of a large molecule in condensed matter consists of overlapping vibronic transitions, we shall single out the contribution from the low frequency (LF) OA vibrations $\{\omega_s\}$ to $W_j(\mathbf{Q})$: $W_j(\mathbf{Q}) = W_{jM} + W_{js}$ where W_{js} is the Hamiltonian governing the nuclear degrees of freedom of the LFOA molecular vibrations, and W_{jM} is the Hamiltonian representing the nuclear degrees of freedom of the HFOA vibrations of a molecule.

The influence of the vibrational subsystems of molecule m on the electronic transition within the range of definite vibronic transition related to HFOA vibration ($\approx 1000 - 1500\text{cm}^{-1}$) can be described as a modulation of this transition by LFOA vibrations $\{\omega_s\}$.³³ We suppose that $\hbar\omega_s \ll k_B T$. Thus $\{\omega_s\}$ is an almost classical system. In accordance with the Franck-Condon principle, an optical electronic transition takes place at a fixed nuclear configuration. Therefore, the quantity $u_{1s}(\mathbf{Q}) = W_{2s}(\mathbf{Q}) - W_{1s}(\mathbf{Q}) - \langle W_{2s}(\mathbf{Q}) - W_{1s}(\mathbf{Q}) \rangle_1$ representing electron-vibration coupling is the disturbance of nuclear motion under electronic transition where $\langle \rangle_j$ stands for the trace operation over the reservoir variables in the electronic state j . Electronic transition relaxation stimulated by LFOA vibrations is described by the correlation function $K_m(t) = \langle \alpha_m(0)\alpha_m(t) \rangle$ of the corresponding vibrational disturbance with characteristic attenuation time τ_s ^{32,34,35} where $\alpha_m \equiv -u_{1s}/\hbar$. In other words, LFOA vibrations lead to a stochastic modulation of the frequency of electronic transition $1 \rightarrow 2$ of molecule m according to

$\tilde{\omega}_{21}(t) = \omega_{21} - \alpha_m(t)$ where $\omega_{21} = [(E_2 - E_1) + \langle W_{2s}(\mathbf{Q}) - W_{1s}(\mathbf{Q}) \rangle_1]/\hbar$ is the frequency of Franck-Condon transition $1 \rightarrow 2$, and $\alpha_m(t)$ is assumed to be Gaussian-Markovian process with $\langle \alpha_m(t) \rangle = 0$ and exponential correlation function $K_m(t) = K(t) = K(0)\exp(-|t|/\tau_s)$. For brevity, we consider first a single vibronic transition related to a HFOA vibration. Generalization to the case of a number of vibronic transitions with respect to a HFOA vibration will be made later.

Consider the expectation value of excitonic operator b_m

$$\langle b_m(\alpha) \rangle \equiv \text{Tr}[b_m \rho_m(\alpha, t)] \quad (12)$$

where $\rho_{m,ij}(\alpha, t)$ is the partial density matrix of molecule m .^{28,36,37} Diagonal elements of the density matrix $\rho_{m,jj}(\alpha, t)$ describe the molecule distribution in states 1 and 2 with a given value of α at time t . The complete density matrix averaged over the stochastic process which modulates the molecule energy levels, is obtained by integration of $\rho_{m,ij}(\alpha, t)$ over α , $\langle \rho_m \rangle_{ij}(t) = \int \rho_{m,ij}(\alpha, t) d\alpha$, where quantities $\langle \rho_m \rangle_{jj}(t)$ are the normalized populations of the corresponding electronic states: $\langle \rho_m \rangle_{jj}(t) \equiv n_{m,j}$, $n_{m,1} + n_{m,2} = 1$. Combining Eqs.(6) and (12), one can introduce the expectation value of $b_{\mathbf{k}}$

$$\langle b_{\mathbf{k}}(\alpha) \rangle = \frac{1}{\sqrt{N}} \sum_m \langle b_m(\alpha) \rangle \exp(-i\mathbf{k} \cdot \mathbf{r}_m) \quad (13)$$

where $\langle b_m(\alpha) \rangle = \rho_{m,21}(\alpha, t)$,^{28,38} and averaging in the density matrix is carry out with respect to the vibrational subsystem of the m -th molecule.

Let us write the equation for the expectation value of $b_{\mathbf{k}}$ corresponding to operator equation (11). If one considers only intramolecular vibrations, \hat{H}_{int} gives the following contribution to the change of the expectation value of excitonic operator b_m in time in the site-representation²⁸

$$\begin{aligned} \frac{\partial}{\partial t} \langle b_m(\alpha) \rangle &\sim \frac{i}{\hbar} \langle [\hat{H}_{int}, b_m] \rangle \equiv \frac{i}{\hbar} \text{Tr}([\hat{H}_{int}, b_m] \rho) = \\ &-i \sum_{n \neq m} J_{mn} \langle \hat{n}_{m1}(\alpha) - \hat{n}_{m2}(\alpha) \rangle \langle b_n \rangle \end{aligned} \quad (14)$$

where $\hat{n}_{m1} = b_m b_m^\dagger$, $\hat{n}_{m2} = b_m^\dagger b_m$ is the exciton population operator, $\langle n_{m1}(\alpha) \rangle = \rho_{m,11}(\alpha, t)$, and

$\langle n_{m2}(\alpha) \rangle = \rho_{m,22}(\alpha, t)$ may be neglected for weak excitation. Here $\langle b_n \rangle = \int \langle b_n(\alpha) \rangle d\alpha = \int \rho_{n,21}(\alpha, t) d\alpha$ is the complete density matrix averaged over the stochastic process.

We emphasize that factorization adopted in Eq.(14) corresponded to neglect of all correlations among different molecules.²⁸ At the same time the factorization corresponds to a random phase approximation³⁹ that enables us to split the term $\langle (\hat{n}_{m1} - \hat{n}_{m2})b_n \rangle$ into the product of populations and polarization ($\langle b_n \rangle$). It is in this sense that the factorization can be understood in the momentum representation.

Furthermore, neglecting $b_{\mathbf{k}'}^\dagger b_{\mathbf{k}}$ in Eq.(10) for weak excitation, one can write $b_{\mathbf{k}'}^\dagger b_{\mathbf{k}}^\dagger \simeq \delta_{\mathbf{k}\mathbf{k}'}$ or

$$b_{\mathbf{k}'}^\dagger b_{\mathbf{k}}^\dagger - b_{\mathbf{k}}^\dagger b_{\mathbf{k}'}^\dagger \simeq \hat{n}_{1\mathbf{k}} \delta_{\mathbf{k}\mathbf{k}'} \quad (15)$$

where $\hat{n}_{1\mathbf{k}} \simeq 1$. Using Eq.(14) and Eqs.(6), (7), (8), (9), (13) and (15), we get

$$\frac{\partial}{\partial t} \langle b_{\mathbf{k}}(\alpha) \rangle \sim -iJ(\mathbf{k}) \langle b_{\mathbf{k}} \rangle \rho_{11}^{(0)}(\alpha) \quad (16)$$

where $\langle b_{\mathbf{k}} \rangle = \int \langle b_{\mathbf{k}}(\alpha) \rangle d\alpha$ and $\rho_{11}^{(0)}(\alpha)$ is the equilibrium value of $\rho_{11}(\alpha)$.

Eq.(16) describes the contribution of \hat{H}_{int} to the change of the expectation value $\langle b_{\mathbf{k}}(\alpha) \rangle$ in time in the momentum representation. In addition, the change of $\langle b_{\mathbf{k}}(\alpha) \rangle$ is determined by the vibrational relaxation. If one considers an absorption experiment and the corresponding polariton problem, the relevant vibrational relaxation occurs in the ground electronic state. In that case the density matrix of a monomer molecule $\rho_{m,21}(\alpha, t) = \langle b_m(\alpha) \rangle$ obeys the equation^{28,36,37,40-42}

$$\begin{aligned} & \left[\frac{\partial}{\partial t} + i(\omega_{21} - \alpha) - L_{11} \right] \rho_{m,21}(\alpha, t) \\ &= \frac{i}{2\hbar} \mathbf{D}_{21} \cdot \mathbf{e}_{\mathbf{q}} \mathcal{E}_{\mathbf{q}} \exp[i(\mathbf{q} \cdot \mathbf{r}_m - \omega_{\mathbf{q}} t)] \rho_{m,11}^{(0)}(\alpha) \end{aligned} \quad (17)$$

where operator

$$L_{11} = \tau_s^{-1} \left[1 + \alpha \frac{\partial}{\partial \alpha} + K(0) \frac{\partial^2}{\partial \alpha^2} \right] \quad (18)$$

describes the diffusion with respect to coordinate α in the effective parabolic potential $U_1(\alpha)$.

Bearing in mind that $\langle b_m(\alpha) \rangle = \rho_{m,21}(\alpha, t)$, we multiply both sides of Eq.(17) by $\exp(-i\mathbf{k} \cdot \mathbf{r}_m)$ and sum with respect to m . As a result we get

$$\begin{aligned} & \left[\frac{\partial}{\partial t} + i(\omega_{21} - \alpha) - L_{11} \right] \langle b_{\mathbf{k}}(\alpha) \rangle \\ &= \frac{i}{2\hbar} \sqrt{N} \mathbf{D}_{21} \cdot \mathbf{e}_{\mathbf{k}} \mathcal{E}_{\mathbf{k}} \exp(-i\omega_{\mathbf{k}} t) \rho_{11}^{(0)}(\alpha) \end{aligned} \quad (19)$$

where we used formula $\sum_m \exp[i(\mathbf{q} - \mathbf{k}) \cdot \mathbf{r}_m] = N \delta_{\mathbf{q}\mathbf{k}}$.^{11,31}

Combining Eqs.(16) and (19), we finally get

$$\begin{aligned} & \left[\frac{\partial}{\partial t} + i(\omega_{21} - \alpha) - L_{11} \right] \langle b_{\mathbf{k}}(\alpha) \rangle \\ &= i \left[\frac{\sqrt{N}}{2\hbar} \mathbf{D}_{21} \cdot \mathbf{e}_{\mathbf{k}} \mathcal{E}_{\mathbf{k}} \exp(-i\omega_{\mathbf{k}} t) - J(\mathbf{k}) \langle b_{\mathbf{k}} \rangle \right] \rho_{11}^{(0)}(\alpha) \end{aligned} \quad (20)$$

2.1 Solution of Eq.(20)

Consider first the slow modulation limit when $K(0)\tau_s^2 \gg 1$. In that case the term L_{11} on the left-hand side of Eq.(20) can be discarded,^{28,37,41} and we get

$$\begin{aligned} \frac{\partial}{\partial t} \langle \tilde{b}_{\mathbf{k}}(\alpha) \rangle &= -i(\omega_{21} - \omega_{\mathbf{k}} - \alpha) \langle \tilde{b}_{\mathbf{k}}(\alpha) \rangle + i \left[\frac{\sqrt{N}}{2\hbar} \times \right. \\ & \quad \left. \times \mathbf{D}_{21} \cdot \mathbf{e}_{\mathbf{k}} \mathcal{E}_{\mathbf{k}} - J(\mathbf{k}) \langle \tilde{b}_{\mathbf{k}} \rangle \right] \rho_{11}^{(0)}(\alpha) \end{aligned} \quad (21)$$

where $\langle \tilde{b}_{\mathbf{k}}(\alpha) \rangle = \langle b_{\mathbf{k}}(\alpha) \rangle \exp(i\omega_{\mathbf{k}} t)$. In the steady-state regime, Eq.(21) leads to

$$\langle \tilde{b}_{\mathbf{k}} \rangle = \frac{i\pi W_a(\omega_{\mathbf{k}}) \frac{\sqrt{N}}{2\hbar} \mathbf{D}_{21} \cdot \mathbf{e}_{\mathbf{k}} \mathcal{E}_{\mathbf{k}}}{1 + i\pi W_a(\omega_{\mathbf{k}}) J(\mathbf{k})} \quad (22)$$

where

$$W_a(\omega_{\mathbf{k}}) = i \int_{-\infty}^{\infty} d\alpha \rho_{11}^{(0)} \zeta(\omega_{\mathbf{k}} - \omega_{21} + \alpha) / \pi, \quad (23)$$

is the monomer spectrum, $\zeta(\omega_{\mathbf{k}} - \omega_{21} + \alpha) = \frac{P}{\omega_{\mathbf{k}} - \omega_{21} + \alpha} - i\pi \delta(\omega_{\mathbf{k}} - \omega_{21} + \alpha)$, P is the symbol of the principal value. The imaginary part of " $-iW_a(\omega_{\mathbf{k}})$ " with sign minus, $-\text{Im}[-iW_a(\omega_{\mathbf{k}})] = \text{Re}W_a(\omega_{\mathbf{k}}) \equiv F_a(\omega_{\mathbf{k}})$, describes the absorption lineshape of a monomer molecule, and

the real part, $\text{Re}[-iW_a(\omega_{\mathbf{k}})] = \text{Im}W_a(\omega_{\mathbf{k}})$, describes the corresponding refraction spectrum. For the "slow modulation" limit, quantities $W_a(\omega_{\mathbf{k}})$ and $F_a(\omega_{\mathbf{k}})$ are given by

$$W_a(\omega_{\mathbf{k}}) = \sqrt{\frac{1}{2\pi K(0)}} w\left(\frac{\omega_{\mathbf{k}} - \omega_{21}}{\sqrt{2K(0)}}\right) \quad (24)$$

where $w(z) = \exp(-z^2)[1 + i\text{erfi}(z)]$ is the probability integral of a complex argument,⁴³ and

$$F_a(\omega_{\mathbf{k}}) = \sqrt{\frac{1}{2\pi K(0)}} \exp\left[-\frac{(\omega_{21} - \omega_{\mathbf{k}})^2}{2K(0)}\right] \quad (25)$$

It might be well to point out that the magnitude $W_a(\omega_{\mathbf{k}})$ is proportional to the molecular polarizability, and the expression in the square brackets on the right-hand side of Eq.(21) may be considered as the interaction with the local field in the \mathbf{k} -space divided by \hbar . Therefore, Eq.(22) can be used also beyond the slow modulation limit when $W_a(\omega_{\mathbf{k}})$ is given by^{40,44} (see Section 1 of the Supporting Information)

$$W_a(\omega_{\mathbf{k}}) = \frac{\tau_s}{\pi} \frac{\Phi(1, 1 + x_a; K(0)\tau_s^2)}{x_a} \quad (26)$$

where $x_a = K(0)\tau_s^2 + i\tau_s(\omega_{21} - \omega_{\mathbf{k}})$, $\Phi(1, 1 + x_a; K(0)\tau_s^2)$ is a confluent hypergeometric function.⁴³ In that case one cannot neglect the term L_{11} describing relaxation in the ground electronic state (see Section 1 of the Supporting Information). In this relation one should note the following. The "slow modulation" limit, Eqs. (24) and (25), is correct only near the absorption maximum. The wings decline much slower as $(\omega_{21} - \omega_{\mathbf{k}})^{-4}$.⁴⁰ At the same time, the expression for $\langle \tilde{b}_{\mathbf{k}} \rangle$, Eq.(22), has a pole, giving strong increasing $\langle \tilde{b}_{\mathbf{k}} \rangle$, when $1/[J(\mathbf{k})\pi] = \text{Im}W_a(\omega_{\mathbf{k}})$. If parameter of the dipole-dipole intermolecular interaction $|J(\mathbf{k})|$ is rather large, the pole may be at a large distance from the absorption band maximum where the "slow modulation" limit breaks down. This means one should use exact expression for the monomer spectrum W_a that is not limited by the "slow modulation" approximation, and properly describes both the central spectrum region and its wings.²⁸ Eq.(26) is the exact expression for the Gaussian-Markovian

modulation with the exponential correlation function $K(t) = K(0) \exp(-|t|/\tau_s)$.

Moreover, we can take also HFOA intramolecular vibrations into account, in addition to the LFOA vibrations $\{\omega_s\}$ discussed thus far. In that case $W_a(\omega_{\mathbf{k}})$ is given by²⁸ (see Section 2 of the Supporting Information)

$$W_a(\omega_{\mathbf{k}}) = \frac{\tau_s}{\pi} \exp(-S_0 \coth \theta_0) \sum_{l=-\infty}^{\infty} I_l\left(\frac{S_0}{\sinh \theta_0}\right) \times \exp(l\theta_0) \frac{\Phi(1, 1 + x_{al}; K(0)\tau_s^2)}{x_{al}} \quad (27)$$

where $x_{al} = K(0)\tau_s^2 + i\tau_s(\omega_{21} - \omega_{\mathbf{k}} + l\omega_0)$. We consider one normal HF intramolecular oscillator of frequency ω_0 whose equilibrium position is shifted under electronic transition, and S_0 is the dimensionless parameter of the shift, $\theta_0 = \hbar\omega_0/(2k_B T)$, $I_l(x)$ is the modified Bessel function of first kind.⁴³

Eq.(27) is the extension of Eq.(26) to the presence of the HFOA intramolecular vibrations. For $\theta_0 \gg 1$ we obtain

$$W_a(\omega_{\mathbf{k}}) = \frac{\tau_s}{\pi} \exp(-S_0) \sum_{l=0}^{\infty} \frac{S_0^l}{l!} \frac{\Phi(1, 1 + x_{al}; K(0)\tau_s^2)}{x_{al}} \quad (28)$$

3 Polarization, Susceptibility and Dielectric Function in \mathbf{k} -Space

The positive frequency component of the polarization per unit volume at point \mathbf{r} can be written as

$$\mathbf{P}^+(\mathbf{r}, t) = N\mathbf{D}_{12}\langle b_m \rangle = \mathbf{P}(\mathbf{k}, \omega_{\mathbf{k}}) \exp[i(\mathbf{k} \cdot \mathbf{r} - \omega_{\mathbf{k}}t)] \quad (29)$$

where

$$\mathbf{P}(\mathbf{k}, \omega_{\mathbf{k}}) = N\mathbf{D}_{12} \frac{1}{\sqrt{N}} \langle \tilde{b}_{\mathbf{k}} \rangle = \frac{N\mathbf{D}_{12}}{2\hbar} \frac{i\pi W_a(\omega_{\mathbf{k}}) \mathbf{D}_{21} \cdot \mathbf{e}_{\mathbf{k}} \mathcal{E}_{\mathbf{k}}}{1 + i\pi W_a(\omega_{\mathbf{k}}) J(\mathbf{k})} \quad (30)$$

N is the density of molecules, and we used Eqs.(9) and (22).

Knowing $\mathbf{P}(\mathbf{k}, \omega_{\mathbf{k}})$, one can calculate the susceptibility

$$\chi(\mathbf{k}, \omega_{\mathbf{k}}) = \frac{N\mathbf{D}_{12}\mathbf{D}_{21}}{\hbar} \frac{i\pi W_a(\omega_{\mathbf{k}})}{1 + i\pi W_a(\omega_{\mathbf{k}})J(\mathbf{k})} \quad (31)$$

and the dielectric function $\varepsilon(\mathbf{k}, \omega_{\mathbf{k}}) = \varepsilon_0[1 + 4\pi\chi(\mathbf{k}, \omega_{\mathbf{k}})]$ ³⁹

$$\varepsilon(\mathbf{k}, \omega_{\mathbf{k}}) = \varepsilon_0[1 + 4\pi \frac{N\mathbf{D}_{12}\mathbf{D}_{21}}{\hbar} \frac{i\pi W_a(\omega_{\mathbf{k}})}{1 + i\pi W_a(\omega_{\mathbf{k}})J(\mathbf{k})}] \quad (32)$$

where $\varepsilon_0 = n_0^2$, n_0 is the background refractive index of the medium, and the vector product in the numerator of Eqs.(31) and (32) is a dyadic product.

If we assume for simplicity that the excitons have an isotropic effective mass, then

$$J(\mathbf{k}) = J(0) + \frac{\hbar \mathbf{k}^2}{2m^*} \quad (33)$$

where the exciton effective mass, m^* , may be both positive and negative. One can see that the susceptibility, Eq.(31), has a pole when the imaginary part of the monomer spectrum, $\text{Im}W_a(\omega_{\mathbf{k}})$, is equal to $1/[J(\mathbf{k})\pi]$, i.e. at the frequency of the exciton with the same wave vector as the exciting field. In other words, we deal with spatial dispersion. It is worth noting that the structure of the dispersion curves $J(\mathbf{k})$ occurs on the scale of $|\mathbf{k}| \sim (0.1 - 1 \text{ nm})^{-1}$, which is much larger than the scale of an optical wave vector. For this reason in practice one may often neglect the spatial dispersion and simply calculate the exciton resonances for $J(0)$, as we did in Ref.²⁸ and where we obtained a good agreement between theoretical and experimental absorption spectra of H-aggregates. In contrast, spatial dispersion may be of importance for J -aggregates due to small bandwidth of their spectra, and also in microcavities where the exciton effective mass may be much smaller than electron mass,¹¹ and then the second term on the right-hand side of Eq.(33) strongly increases. Fig.1 shows the absorption spectra of a J -aggregate that are proportional to the imaginary part of the susceptibility $\text{Re} \frac{W_a(\omega_{\mathbf{k}})}{1 + i\pi W_a(\omega_{\mathbf{k}})J(\mathbf{k})}$, Eq.(33), calculated for $J(\mathbf{k}) = J(0)$ ²⁸ (solid line), and for $J(\mathbf{k}) = J(0) + \frac{\hbar \mathbf{k}^2}{2m^*}$

Figure 1: Absorption spectra (in terms of τ_s/π) of a J -aggregate calculated for $J(\mathbf{k}) = J(0)$ (solid line), and $J(\mathbf{k}) = J(0) + \frac{\hbar \mathbf{k}^2}{2m^*}$ (dashed line) in the case of slow modulation ($\sqrt{K(0)}\tau_s = 10.9 \gg 1$) and $-J(0)\tau_s = 42$. Dimensionless parameter is $\delta = \tau_s(\omega_{\mathbf{k}} - \omega_{21})$. Other parameters are $m^* = 0.1m_{el}$, m_{el} is the electron mass, $|\mathbf{k}| = n2\pi/\lambda$, $n = 3.16$ is the refraction index, $\lambda = 0.5 \mu$.

(dashed line). The monomer spectrum $W_a(\omega_{\mathbf{k}})$ is calculated using Eq.(26). One can see that due to small bandwidth of the J -aggregate absorption with respect to that of the monomer (see Fig.1 of Ref.²⁸), the spatial dispersion can lead to marked broadening the J -aggregate spectrum. In contrast, the role of the spatial dispersion may be overestimated in works not considering the vibrational contribution.^{3,45}

4 Luminescence

In this section we shall use our mean-field theory for the calculation of the relaxed luminescence of aggregates for weak excitation. To describe this process, we shall consider a quantum electromagnetic field of the spontaneous emission

$$\mathbf{E}_s(\mathbf{r}, t) = \frac{1}{2}\mathbf{e}_s\mathcal{E}_s \exp(\mathbf{k}_s\mathbf{r}-i\omega_s t) + \frac{1}{2}\mathbf{e}_s^*\mathcal{E}_s^\dagger \exp(\mathbf{k}_s\mathbf{r}-i\omega_s t) \quad (34)$$

in addition to the incident classical field of frequency ω . Eq.(34) is Eq.(4) for $\mathbf{q} = \mathbf{k}_s$. This process is depicted by the double-sided Feynman diagrams^{32,41,46} where due to condensed matter the light-matter interaction described by the Rabi frequency, $\Omega_R = (\mathbf{D} \cdot \mathbf{e}_{\mathbf{k}})\mathcal{E}_{\mathbf{k}}/\hbar$, should be replaced by the effective Rabi frequency, $\Omega_{eff}(t) = \Omega_R/[1 + i\pi W_a(\omega_{\mathbf{k}})J(0)]$ ²⁸ (see also Section 3).

In the site representation the photon emission rate of mode \mathbf{k} obeys the equation

$$\begin{aligned} \frac{\partial}{\partial t}\langle a_{\mathbf{k}}^\dagger a_{\mathbf{k}} \rangle &= \frac{i}{\hbar}\langle [-(\hat{\mathbf{D}} \cdot \hat{\mathbf{E}})_{eff}, a_{\mathbf{k}}^\dagger a_{\mathbf{k}}] \rangle = 2\frac{\sqrt{2\pi\hbar\omega_{\mathbf{k}}}}{\hbar}\mathbf{D} \\ &\times \sum_m \text{Re} \frac{\langle a_{\mathbf{k}}^\dagger \tilde{b}_m \rangle u_{\mathbf{k}}^*(\mathbf{r})}{1 - i\pi W_a^*(\omega_{\mathbf{k}})J(0)} \end{aligned} \quad (35)$$

Figure 2: Double sided Feynman diagrams for relaxed luminescence.

where in general the trace in this expression is over the vibrational as well as the field degrees of freedom, and we used relation $\mathbf{e}_{\mathbf{q}}\mathcal{E}_{\mathbf{q}} \exp(i\mathbf{q} \cdot \mathbf{r}) = i2\sqrt{2\pi\hbar\omega_{\mathbf{q}}}a_{\mathbf{q}}u_{\mathbf{q}}(\mathbf{r})$ between the amplitude of electric field, $\mathcal{E}_{\mathbf{q}}$, and the annihilation operator for mode \mathbf{q} , $a_{\mathbf{q}}$. Here $\tilde{b}_m = b_m \exp(i\omega_{\mathbf{k}}t)$ and $\langle b_m \rangle = \rho_{m,21}$ that should be calculated in the third order with respect to the light-matter interaction (see Fig. 2).

Diagrams (1) and (2) of Fig.2 give contributions into $\langle \rho_{21}^{(3)} \rangle$. Adopting for a while the picture of fast vibrational relaxation when the equilibrium distribution into the excited electronic state has had time to be set during the lifetime of this state, one gets for the contribution described by the lower parts of these diagrams

$$\rho_{22}(\alpha) = \frac{n_2^{(2)}}{(2\pi K(0))^{1/2}} \exp\left[-\frac{(\alpha - \omega_{st})^2}{2K(0)}\right] \quad (36)$$

where $n_2^{(2)} \ll 1$ is the population of excited electronic state 2 calculated in the second order with respect to electromagnetic field and $\omega_{st} = \hbar K(0)/k_B T$ is the Stokes shift of the equilibrium absorption and luminescence spectra.

Consider equation for nondiagonal density matrix in the site representation related to the upper parts of diagrams (1) and (2) of Fig.2

$$\begin{aligned} & \left[\frac{\partial}{\partial t} + i(\omega_{21} - \alpha) - L_{22} \right] \rho_{21}(\alpha, t) \\ &= \frac{i}{2\hbar} \mathbf{D}_{21} \cdot \mathbf{e} \mathcal{E}_{\mathbf{q}} \exp[i(\mathbf{q} \cdot \mathbf{r} - \omega_{\mathbf{q}} t)] \rho_{22}(\alpha) \\ & \quad - iJ(0) \rho_{11}^{(0)}(\alpha) \int \rho_{21}(\alpha, t) d\alpha \end{aligned} \quad (37)$$

where operator

$$L_{22} = \tau_s^{-1} \left[1 + \frac{(\alpha - \omega_{st})}{\partial(\alpha - \omega_{st})} \frac{\partial}{\partial(\alpha - \omega_{st})} + \frac{\sigma_{2s} \partial^2}{\partial(\alpha - \omega_{st})^2} \right]$$

describes the diffusion with respect to coordinate α in the excited electronic state. The latter and the presence of $\rho_{22}(\alpha)$ in the first term on the right-hand-side of Eq.(37) are distinctions of Eq.(37) from the corresponding equation related to absorption, Eq.(17). In contrast, the last term on the right-hand-side of Eq.(37) is the same as in the case of absorption (the presence of $\rho_{11}^{(0)}(\alpha)$). The fact is that this term describes the local field effects due to polarization of other molecules that are found in the main in the ground electronic state.

Eq.(37) can be solved similar to the equation for absorption (see Section 1 of the Supporting Information). The homogeneous equation obtained from

Eq.(37) can be reduced to Eq.(1) of the Supporting Information using notation $\alpha_2 = \alpha - \omega_{st}$ with the only difference that ω_{21} should be replaced by $\omega_{21} - \omega_{st}$. Then we obtain for the line shape of a monomer fluorescence

$$W_f(\omega_{\mathbf{k}}) = \frac{1}{\pi} \int_0^\infty \exp[i(\omega_{\mathbf{k}} - \omega_{21} + \omega_{st})t + g_s(t)] dt \quad (38)$$

instead of Eq.(5) of the Supporting Information, and

$$W_f(\omega_{\mathbf{k}}) = \frac{\tau_s}{\pi} \frac{\Phi(1, 1 + x_f; K(0)\tau_s^2)}{x_f} \quad (39)$$

instead of Eq.(26) where $x_f = K(0)\tau_s^2 + i\tau_s(\omega_{21} - \omega_{st} - \omega_{\mathbf{k}})$.

When one include also HFOA intramolecular vibrations (see Section 2 of the Supporting Information), the formula becomes

$$\begin{aligned} W_f(\omega_{\mathbf{k}}) &= \frac{\tau_s}{\pi} \exp(-S_0 \coth \theta_0) \sum_{l=-\infty}^{\infty} I_l \left(\frac{S_0}{\sinh \theta_0} \right) \\ & \quad \times \exp(l\theta_0) \frac{\Phi(1, 1 + x_{fl}; K(0)\tau_s^2)}{x_{fl}} \end{aligned} \quad (40)$$

where $x_{fl} = K(0)\tau_s^2 + i\tau_s(\omega_{21} - \omega_{st} - \omega_{\mathbf{k}} - l\omega_0)$. For $\theta_0 \gg 1$ we obtain

$$W_f(\omega_{\mathbf{k}}) = \frac{\tau_s}{\pi} \exp(-S_0) \sum_{l=0}^{\infty} \frac{S_0^l}{l!} \frac{\Phi(1, 1 + x_{fl}; K(0)\tau_s^2)}{x_{fl}} \quad (41)$$

Then we get for $\langle \tilde{b}_m \rangle = \langle \tilde{\rho}_{21}^{(3)} \rangle = \langle \rho_{21}^{(3)} \rangle \exp(i\omega_{\mathbf{k}} t)$

$$\langle \tilde{b}_m \rangle = -\frac{1}{\hbar} \sqrt{2\pi\hbar\omega_{\mathbf{k}}} a_{\mathbf{k}} \mathbf{D}_{21} \cdot \mathbf{u}_{\mathbf{k}}(\mathbf{r}) n_2^{(2)} \frac{\pi W_f(\omega_{\mathbf{k}})}{1 + i\pi J(0) W_a(\omega_{\mathbf{k}})} \quad (42)$$

Substituting Eq.(42) into Eq.(35), we obtain

$$\frac{\partial}{\partial t} \langle a_{\mathbf{k}}^\dagger a_{\mathbf{k}} \rangle = -\frac{4\pi^2}{\hbar^2 V} \hbar \omega_{\mathbf{k}} (\mathbf{D}_{12} \cdot \mathbf{e}_{\mathbf{k}}) \sum_m n_2^{(2)} \text{Re} \frac{\langle a_{\mathbf{k}}^\dagger a_{\mathbf{k}} \rangle (\mathbf{D}_{21} \cdot \mathbf{e}_{\mathbf{k}}) W_f(\omega_{\mathbf{k}})}{|1 + i\pi W_a(\omega_{\mathbf{k}}) J(0)|^2} \quad (43)$$

where the fluorescence line shape of an exciton is given by

$$F_{exc,f}(\omega_{\mathbf{k}}) = \text{Re} \frac{W_f(\omega_{\mathbf{k}})}{|1 + i\pi W_a(\omega_{\mathbf{k}})J(0)|^2} \quad (44)$$

and

$$n_2^{(2)} = \langle b_m^\dagger b_m \rangle^{(2)} \quad (45)$$

In deriving Eq.(43) we neglected the correlation between fluorescence photons and the medium polarization. Therefore, Eq.(43) describes the exciton luminescence. The polariton luminescence can be obtained in terms of the expectation values of $\langle a_{\mathbf{k}}^\dagger a_{\mathbf{k}'} \rangle$, $\langle a_{\mathbf{k}}^\dagger \tilde{b}_m \rangle$, $\langle \tilde{b}_m^\dagger \tilde{b}_n \rangle$ *etc.*⁴⁷ satisfying coupled equations of motion and will be considered elsewhere.

It should be noted that the exciton luminescence, Eq.(44), and absorption

$$\begin{aligned} F_{exc,a}(\omega_{\mathbf{k}}) &= \text{Re} \frac{W_a(\omega_{\mathbf{k}})}{1 + i\pi W_a(\omega_{\mathbf{k}})J(0)} \\ &= \text{Re} \frac{W_a(\omega_{\mathbf{k}})}{|1 + i\pi W_a(\omega_{\mathbf{k}})J(0)|^2} \end{aligned} \quad (46)$$

spectra obey Stepanov's law^{11,30} if the corresponding monomer spectra obey this relation. Indeed, if $\text{Re} W_f(\omega_{\mathbf{k}}) = \text{Re} W_a(\omega_{\mathbf{k}}) \exp[-\hbar(\omega_{\mathbf{k}} - \omega_{el})/k_B T]$ where $\omega_{el} = (E_2 - E_1)/\hbar$ is the frequency of a purely electronic transition, then

$$F_{exc,f}(\omega_{\mathbf{k}}) = F_{exc,a}(\omega_{\mathbf{k}}) \exp[-\hbar(\omega_{\mathbf{k}} - \omega_{el})/k_B T] \quad (47)$$

Fig.3 shows absorption and fluorescence spectra of a *J*-aggregate calculated using Eqs. (46) and (44), respectively. The monomer spectra $W_a(\omega_{\mathbf{k}})$ and $W_f(\omega_{\mathbf{k}})$ were calculated using Eqs. (26) and (39), respectively. One can see that the position of the luminescence spectrum is determined in the main by the pole of the denominator on the right-hand-side of Eq.(44) that is about the same as for absorption. That is why the positions of the *J*-aggregate luminescence and absorption spectra coincide, according to experiment, in spite of the Stokes shift of the corresponding monomer spectra (see Fig.3). We emphasize that both narrowing the *J*-aggregate spectra and

Figure 3: Absorption (solid) and relaxed luminescence (dash) spectra of a *J*-aggregate for $\sqrt{K(0)}\tau_s = 3.16$, $\tau_s = 10^{-13}$ s and $-J(0)\tau_s = 5$. The monomer absorption (dots) and luminescence (dash-dot) are shown for comparison.

diminishing their Stokes shift with respect to those of a monomer covered by our non-Markovian theory cannot be described by the model of a single HFOA vibration.^{25,27} We shall apply the theory of this section to H-aggregates below.

4.1 Exciton luminescence in k -space

Consider an exciton luminescence in the \mathbf{k} -space. Using Eq.(45), and bearing in mind that $\sum_m b_m^\dagger b_m = \sum_{\mathbf{k}'} b_{\mathbf{k}'}^\dagger b_{\mathbf{k}'}$ and that the translational symmetry of a perfect bulk crystal implies that excitons of wave vector \mathbf{k} can only couple to electromagnetic waves of the same wave vector, we get from Eq.(43)

$$\begin{aligned} \frac{\partial}{\partial t} \langle a_{\mathbf{k}}^\dagger a_{\mathbf{k}} \rangle &= -\frac{4\pi^2}{\hbar^2 V} \hbar \omega_{\mathbf{k}} (\mathbf{D}_{12} \cdot \mathbf{e}_{\mathbf{k}}) \langle b_{\mathbf{k}}^\dagger b_{\mathbf{k}} \rangle^{(2)} \\ &\times \text{Re} \frac{\langle a_{\mathbf{k}}^\dagger a_{\mathbf{k}} \rangle (\mathbf{D}_{21} \cdot \mathbf{e}_{\mathbf{k}}) W_f(\omega_{\mathbf{k}})}{|1 + i\pi W_a(\omega_{\mathbf{k}}) J(\mathbf{k})|^2} \end{aligned} \quad (48)$$

Let us suppose a thermal equilibrium in the \mathbf{k} -space

$$\langle b_{\mathbf{k}}^\dagger b_{\mathbf{k}} \rangle^{(2)} \sim \frac{\exp[-J(\mathbf{k})/k_B T]}{\sum_{\mathbf{k}} \exp[-J(\mathbf{k})/k_B T]} \quad (49)$$

and assume for simplicity that the excitons have an isotropic effective mass, Eq.(33). For positive effective mass $J(\mathbf{k})$ may be replaced by $J(0)$ like before, and we arrive to the result obtained in the site-representation. In contrast, for negative effective mass, $J(\mathbf{k}) \approx J(\mathbf{k}_{lum})$ where \mathbf{k}_{lum} corresponds to the minimum of $J(\mathbf{k})$. In that case one can expect an additional red shift of the luminescence spectrum with respect to the vibrational Stokes shift ω_{st} .

5 Application to Exciton-Polariton Experiment in Nanofiber

In this section we apply the theory developed above to the experiment on fraction of a millimeter propagation of EPs in photoexcited fiber-shaped H-aggregates of TC dye at room temperature³ bearing in mind the correspondence between manifestation of

Figure 4: Experimental absorption lineshape of TC monomer solution prepared by dissolving TC dye in methanol¹ (circles), and its fitting by $\text{Re}W_a$, Eq.(28), (solid line).

electron-vibrational interaction in monomers, molecular aggregates and EP dispersion in nanofibers.

Fig. 4 shows the experimental absorption lineshape of TC monomer solution prepared by dissolving TC dye in methanol,¹ and its fitting by $\text{Re}W_a$, Eq.(28) for $\omega_{21} = 23700 \text{ cm}^{-1}$, $1/\tau_s = 75 \text{ cm}^{-1}$, $\omega_0\tau_s = 20$, $S_0 = 0.454$, $K(0)\tau_s^2 = 80$.

Using the last parameters we calculated the aggregate absorption and photoluminescence spectra according to formulas (46) and (44), respectively, shown in Fig.5. Good agreement between theoretical and experimental spectra is observed with the value of parameter $J(0)\tau_s = 7$ obtained by comparison between experimental and theoretical curves. Dimensionless parameter of the Stokes shift is equal to $\omega_{st}\tau_s = \hbar K(0)\tau_s^2/(k_B T\tau_s) = 28.6$ for room temperature ($k_B T/\hbar = 210 \text{ cm}^{-1}$). We did not make additional fitting since experimental spectra of TC aggregates and monomers were measured in different solvents¹ (see caption to Fig.5).

It might be well to point out that both absorption and luminescence H-aggregate spectra were obtained using only one additional parameter $J(0)\tau_s = 7$ with respect to those found by fitting the absorption monomer spectrum. This speaks in favor of the proposed physical model of forming the aggregate spectra.

The description of the aggregate spectra obtained above enables us to get the dielectric function, Eq.(32), and find the transverse eigenmodes of the medium from the dispersion equation

$$c^2 k^2(\omega_{\mathbf{k}}) = \omega_{\mathbf{k}}^2 \varepsilon(\mathbf{k}, \omega_{\mathbf{k}}) \quad (50)$$

Bearing in mind discussion just after Eq.(32), we take the exciton resonances at $J(0)$ (so called $\mathbf{k}=0$ selection rule¹⁰), so that we shall use $\varepsilon(0, \omega) \equiv \varepsilon(\omega)$ in our simulations of EP dispersion. Inclusion of spatial dispersion in Ref.³ to account for line broadening arose from the use a simple Lorentz model that does not take electron-vibrational effects into consideration. Because the fiber in Ref.³ had a rectangular cross section with width of 400-700 nm ($\sim \lambda$) and height of 100-200 nm ($\ll \lambda$), the energy of light guided in the nanofiber was given by

$$\hbar\omega = \sqrt{\hbar^2 c^2 k_{\parallel}^2 + E_C^2/n(\omega)} \quad (51)$$

Figure 5: Experimental absorption and photoluminescence spectra of TC aggregates and monomers¹ (top), and theoretical description of aggregate absorption (in terms of τ_s/π) and photoluminescence (arbitrary units) (bottom). In the top solid curve represents spectra of the aqueous solution containing TC aggregates; dashed curve, spectra of a monomer solution prepared by dissolving TC dye in methanol. In the bottom solid curves represent the aggregate spectra; dashed curves - spectra of a monomer. Dimensionless parameter $\delta = \tau_s(\omega - \omega_{21})$ increases when the wavelength decreases.

where $\mathbf{k}_{||}$ is the wave vector parallel to the fiber and $E_C = \hbar c\pi/d = 1 \text{ eV}$ for $d = 600 \text{ nm}$ is the cutoff energy. Combining Eqs.(50) and (51), we get

$$c^2 k_{||}^2 = \omega^2 \varepsilon(\omega) - \frac{E_C^2}{\hbar^2} \quad (52)$$

Let us analyze Eq.(52) where the dielectric function $\varepsilon(0, \omega) \equiv \varepsilon(\omega)$ is determined by Eq.(32) for $J(\mathbf{k}) = J(0)$. In Ref.²⁸ we considered rather the transverse eigenmodes of the medium, Eq.(50), than the nanofiber modes with wave vector $\mathbf{k}_{||}$. The parameters of the aggregate spectrum were found above. In order to satisfy Eq.(52), the wave number $k_{||}$ should be complex $k_{||} = k'_{||} + ik''_{||}$. Then using Eq.(52), we get for the real and imaginary part of $k_{||}$

$$k'_{||} \frac{c}{n_0} = \omega \text{Re} \sqrt{[1 - \frac{(E_C/\hbar)^2}{\omega^2 \varepsilon_0}] + iq\pi \frac{W_a(\omega)}{1 + i\pi W_a(\omega)J(0)}} \quad (53)$$

and

$$k''_{||} \frac{c}{n_0} = \omega \text{Im} \sqrt{[1 - \frac{(E_C/\hbar)^2}{\omega^2 \varepsilon_0}] + iq\pi \frac{W_a(\omega)}{1 + i\pi W_a(\omega)J(0)}}, \quad (54)$$

respectively, where $q = 4\pi \frac{N\mathbf{D}_{12}\mathbf{D}_{21}}{\hbar}$. Fig.6 shows the Frenkel EP dispersion calculated using Eqs.(53) and (54). The polariton dispersion shows the leaky part in the splitting range between lower and upper polariton branches. The fluorescence spectrum of a nanofiber was in the range of $\sim 2.5 \text{ eV}^3$ where in the main $\text{Im}k_{||} \approx 0$. In addition, the fluorescence spectrum was out of the splitting range under discussion and corresponded to the lower polariton branch due to excitation at $\lambda = 405 \text{ nm}$ below the upper polariton branch. However, if the excitation was at upper polariton branch, photoluminescence from it would be unlikely due to the presence of absorption ($\text{Im}k_{||} \neq 0$) in the range of upper polariton branch (see Fig.6). In contrast, EP emission in materials with narrow absorption lines (J-aggregates) show photoluminescence from both upper and lower polariton branches.^{5,48} It is worth noting that this and other conclusions related to the EP dispersion are based on the correspondence between manifestation of electron-vibrational

Figure 6: Frenkel EP dispersion for real (solid line) and imaginary (dashed line) part of the wave number $k_{||}$ calculated with Eqs.(53) and (54), respectively, when $q\tau_s = 84$.²⁸ Other parameters are identical to those of the bottom of Fig.5.

interaction in monomers, molecular aggregates and EP dispersion in nanofibers. This correspondence is of particular importance when the bandwidth of the imaginary part of the wave vector is of the same order of magnitude as the splitting range between lower and upper polariton branches (see Fig.6).

In this work we have restricted ourselves to the exciton luminescence, Section 4, due to factorization of the term $\langle a_{\mathbf{k}}^\dagger \tilde{b}_m \rangle$ on the right-hand side of Eq.(35) adopted in moving from Eq.(35) to Eq.(43). The factorization enabled us to split the corresponding term on the right-hand side of Eq.(43) into the product of field intensity, $\langle a_{\mathbf{k}}^\dagger a_{\mathbf{k}} \rangle$, and the material term $\sim n_2^{(2)} F_{exc,f}(\omega_{\mathbf{k}})$ where $F_{exc,f}(\omega_{\mathbf{k}})$ is the fluorescence line shape of an exciton, Eq.(44). However, the approach developed in Section 4 can be extended to the polariton luminescence that can be obtained in terms of the expectation values of $\langle a_{\mathbf{k}}^\dagger a_{\mathbf{k}'} \rangle$, $\langle a_{\mathbf{k}}^\dagger \tilde{b}_m \rangle$, $\langle \tilde{b}_m^\dagger \tilde{b}_n \rangle$ etc.⁴⁷ satisfying coupled equations of motion. In contrast to Ref.,⁴⁷ our coupled equations of motion will include non-Markovian relaxation making their solution more complex. This will be done elsewhere.

6 Conclusion

In this work we have developed a model in order to account for electron-vibrational effects on absorption and luminescence of molecular aggregates, and EPs in nanofibers. The model generalizes the mean-field electron-vibrational theory developed by us earlier to the systems with spatial symmetry, exciton luminescence and the EPs with spatial dispersion. The exciton luminescence and absorption spectra in our mean-field theory obey Stepanov's law.^{11,30} Among other things, our theory describes both narrowing the J-aggregate absorption and luminescence spectra, and diminishing the Stokes shift between them with respect to that of a monomer. The correspondence between manifestation of electron-vibrational interaction in monomers, molecular aggregates and EP dispersion in nanofibers is obtained by introducing the aggregate line-shape functions in terms of the monomer line-shape functions. With the same description of material parameters we have calculated both the absorption and luminescence of molecular aggregates, and the EP dispersion in nanofibers. We obtained good agreement between theoretical and experimental absorption and luminescence spectra of both monomers and H-aggregates. We emphasize that both absorption and luminescence H-aggregate spectra were obtained using only one additional parameter with respect to those found by fitting the absorption monomer spectrum. This speaks in favor of the proposed physical model of forming the aggregate spectra. We have applied the theory to experiment on fraction of a millimeter propagation of Frenkel EPs in photoexcited fiber-shaped H-aggregates of TC dye at room temperature³ bearing in mind the correspondence between manifestation of electron-vibrational interaction in monomers, molecular aggregates and EP dispersion in nanofibers.

We have also discussed the extension of our approach to the description of polariton luminescence. This will be done elsewhere.

The theory can be also applied to Frenkel EPs in organic microcavities,^{27,49} to plexcitonics⁵⁰ and the problems related to optics of exciton-plasmon nanomaterials^{51,52} where the rovibrational structure of diatomic molecules was recently included.⁵³ In con-

trast, in our paper we consider a model for aggregates of large organic molecules.

Acknowledgement

This work was supported by the Ministry of Science & Technology of Israel (grant No. 79518). I thank G. Rosenman and B. Apter for useful discussions.

Supporting Information for Publication

Section 1. Contribution of Low Frequency Optically Active Vibrations to Monomer Spectrum

Let $\rho'_{21}(\alpha, t)$ obeys the homogeneous equation that is obtained from inhomogeneous Eq.(17) of the main text. Denoting $\rho'_{21}(\alpha, t) = \bar{\rho}_{21}(\alpha, t) \exp(-i\omega_{21}t)$, we get for $\bar{\rho}_{21}(\alpha, t)$

$$\frac{\partial}{\partial t} \bar{\rho}_{21}(\alpha, t) = \{i\alpha + \tau_s^{-1} [1 + \alpha \frac{\partial}{\partial \alpha} + K(0) \frac{\partial^2}{\partial \alpha^2}]\} \bar{\rho}_{21}(\alpha, t) \quad (55)$$

Introducing the Fourier-transform

$$\begin{aligned} \Psi(\kappa, t) &= \frac{1}{2\pi} \int_{-\infty}^{\infty} \bar{\rho}_{21}(\alpha, t) \exp(-i\kappa\alpha) d\alpha, \\ \bar{\rho}_{21}(\alpha, t) &= \int_{-\infty}^{\infty} \Psi(\kappa, t) \exp(i\kappa\alpha) d\kappa \end{aligned}$$

we get the following equation for $\Psi(\kappa, t)$

$$\frac{\partial \Psi(\kappa, t)}{\partial t} + (\tau_s^{-1} \kappa + 1) \frac{\partial \Psi(\kappa, t)}{\partial \kappa} = -\tau_s^{-1} K(0) \kappa^2 \Psi(\kappa, t) \quad (56)$$

The solution of Eq.(56) is⁴⁰

$$\begin{aligned} \Psi(\kappa, t) &= \exp\left\{-\frac{K(0)}{2} [\kappa^2 + 2\kappa\tau_s(1 - \exp(-t/\tau_s)) + 2\tau_s^2(t/\tau_s - 1 + \exp(-t/\tau_s))]\right\} \end{aligned} \quad (57)$$

with

$$\Psi(0, t) = \exp[g_s(t)] = \frac{1}{2\pi} \int_{-\infty}^{\infty} \bar{\rho}_{21}(\alpha, t) d\alpha$$

playing the role of the characteristic function of absorption spectrum. Here

$$g_s(t) = -K(0)\tau_s^2 [\exp(-t/\tau_s) + \frac{t}{\tau_s} - 1] \quad (58)$$

Indeed, the characteristic function of the absorption spectrum is determined by the free relaxation of the non-diagonal density matrix,⁵⁴ $\rho'_{21}(\alpha, t)$. Then

$$\begin{aligned} W_a(\omega) &= \frac{1}{\pi} \int_0^\infty \exp[i(\omega - \omega_{21})t] \Psi(0, t) dt \\ &= \frac{1}{\pi} \int_0^\infty \exp[i(\omega - \omega_{21})t + g_s(t)] dt \end{aligned} \quad (59)$$

Integrating with respect to t , one gets Eq.(26) of the main text.

Section 2. Including High-Frequency Optically Active Intramolecular Vibrations

Applying Eqs.(46) and (44) of the main text to the description of the absorption and luminescence spectra, respectively, of H-aggregates, one should take into account also high-frequency (HF) optically active (OA) intramolecular vibrations, in addition to the low frequency OA vibrations $\{\omega_s\}$. In that case the corresponding monomer spectra W_a and W_f should include the contribution from the HFOA intramolecular vibrations.²⁸ We consider one normal HF intramolecular oscillator of frequency ω_0 whose equilibrium position is shifted under electronic transition. Its characteristic function $f_{HF}(t)$ is determined by the following expression:^{41,55}

$$\begin{aligned} f_{HF}(t) &= \exp(-S_0 \coth \theta_0) \sum_{k=-\infty}^{\infty} I_k(S_0 / \sinh \theta_0) \\ &\quad \times \exp[k(\theta_0 + i\omega_0 t)] \end{aligned} \quad (60)$$

where S_0 is the dimensionless parameter of the shift, $\theta_0 = \hbar\omega_0/(2k_B T)$, $I_n(x)$ is the modified Bessel function of first kind.⁴³ Then the monomer absorption and luminescence can be written as

$$W_a(\omega) = (1/\pi) \int_0^\infty f_{HF}^*(t) \exp[i(\omega - \omega_{21})t + g_s(t)] dt \quad (61)$$

and

$$W_f(\omega) = (1/\pi) \int_0^\infty f_{HF}(t) \exp[i(\omega - \omega_{21} + \omega_{st})t + g_s(t)] dt, \quad (62)$$

respectively, where $g_s(t)$ is given by Eq.(58). Integrating the last equations with respect to t , one gets Eqs.(27) and (40) of the main text.

Author Information

Corresponding Author

E-mail: fainberg@hit.ac.il

References

- [1] Takazawa, K.; Kitahama, Y.; Kimura, Y.; Kido, G. Optical Waveguide Self-Assembled from Organic Dye Molecules in Solution. *Nano Letters* **2005**, *5*, 1293–1296.
- [2] Takazawa, K. Waveguiding Properties of Fiber-Shaped Aggregates Self-Assembled from Thiacyanine Dye Molecules. *J. Phys. Chem. C* **2007**, *111*, 8671–8676.
- [3] Takazawa, K.; Inoue, J.; Mitsuishi, K.; Takamasu, T. Fraction of a Millimeter Propagation of Exciton Polaritons in Photoexcited Nanofibers of Organic Dye. *Phys. Rev. Letters* **2010**, *105*, 067401.
- [4] Takazawa, K.; Inoue, J.; Mitsuishi, K.; Kuroda, T. Ultracompact Asymmetric Mach-Zehnder Interferometers with High Visibility Constructed from Exciton Polariton Waveguides of Organic Dye Nanofibers. *Advanced Functional Materials* **2013**, *23*, 839–845.
- [5] Ellenbogen, T.; Crozier, K. B. Exciton-Polariton Emission from Organic Semiconductor Optical Waveguides. *Phys. Rev. B* **2011**, *84*, 161304.
- [6] Gentile, M. J.; Nunez-Sanchez, S.; Barnes, W. L. Optical Field-Enhancement and Subwavelength Field-Confinement Using Excitonic Nanostructures. *Nano Letters* **2014**, *14*, 2339–2344.
- [7] Liao, Q.; Xu, Z.; Zhong, X.; Dang, W.; Shi, Q.; Zhang, C.; Weng, Y.; Lid, Z.; Fu, H. An Organic Nanowire Waveguide Exciton-Polariton Sub-Microlaser and Its Photonic Application. *J. Mater. Chem. C* **2014**, *2*, 2773–2778.

- [8] Gather, M. C.; Yun, S. H. Single-Cell Biological Lasers. *Nature Photonics* **2011**, *5*, 406–410.
- [9] Dietrich, C. P.; Steude, A.; Tropsch, L.; Schubert, M.; Kronenberg, N. M.; Ostermann, K.; Hofling, S.; Gather, M. C. An Exciton-Polariton Laser Based on Biologically Produced Fluorescent Protein. *Sci. Adv.* **2016**, *2*, e1600666.
- [10] Knoester, J.; Agranovich, V. M. Frenkel and Charge-Transfer Excitons in Organic Solids. In *Thin Films and Nanostructures: Electronic Excitations in Organic Based Nanostructures*, Vol. 31; Agranovich, V. M.; Bassani, G. F., Eds.; Elsevier Academic Press: Amsterdam, 2003.
- [11] Agranovich, V. M. *Excitations in Organic Solids*; Oxford University Press: New York, 2009.
- [12] Handelman, A.; Lapshina, N.; Apter, B.; Rosenman, G. Peptide Integrated Optics. *Adv. Mater.* **2018**, *30*, 1705776.
- [13] Apter, B.; Lapshina, N.; Handelman, A.; Fainberg, B.D.; Rosenman, G. Peptide Nanophotonics: From Optical Waveguiding to Precise Medicine and Implantable Biochips. *Small* **2018**, 1801147.
- [14] Lapshina, N.; Shishkin, I.; Nandi, R.; Noskov, R.E.; Barhom, H.; Joseph, S.; Apter, B.; Ellenbogen, T.; Natan, A.; Ginzburg P.; et al. Bioinspired Amyloid Nanodots with Visible Fluorescence. *Adv. Opt. Mater.* **2018**, 1801400.
- [15] Joseph, S.K.; Kuritz, N.; Yahel, N.; Lapshina, N.; Rosenman, G.; Natan, A. Proton-transfer induced fluorescence in self assembled short peptides. *J. Phys. Chem. A* **2019**, DOI:10.1021/acs.jpca.8b09183.
- [16] Hopfield, J. J. Theory of the Contribution of Excitons to the Complex Dielectric Constant of Crystals. *Phys. Rev.* **1958**, *112*, 1555–1567.
- [17] Knoester, J.; Mukamel, S. Transient Gratings, Four-Wave Mixing and Polariton Effects in Nonlinear Optics. *Phys. Reports* **1991**, *205*, 1–58.
- [18] Zoubi, H. Collective Interactions in an Array of Atoms Coupled to a Nanophotonic Waveguide. *Phys. Rev. A* **2014**, *89*, 043831.
- [19] Plumhof, J. D.; Stoferle, T.; Mai, L.; Scherf, U.; Mahrt, R. F. Room-Temperature Bose-Einstein Condensation of Cavity Exciton-Polaritons in a Polymer. *Nature Materials* **2014**, *13*, 247–252.
- [20] Lerario, G.; Fieramosca, A.; Barachati, F.; Ballarini, D.; Daskalakis, K. S.; Dominici, L.; Giorgi, M. D.; Maier, S. A.; Gigli, G.; Kena-Cohen, S.; et al. Room-Temperature Superfluidity in a Polariton Condensate. *Nature Physics* **2017**, *13*, 837–841.
- [21] Karzig, T.; Bardyn, C.-E.; Lindner, N. H.; Refael, G. Topological Polaritons. *Phys. Rev. X* **2015**, *5*, 031001.
- [22] Nalitov, A. V.; Solnyshkov, D. D.; Malpuech, G. Polariton Z Topological Insulator. *Phys. Rev. Lett.* **2015**, *114*, 161413.
- [23] Klemmt, S.; Harder, T. H.; Egorov, O. A.; Winkler, K.; Ge, R.; Bandres, M. A.; Emmerling, M.; Worschech, L.; Liew, T. C. H.; Segev, M.; et al. Exciton-Polariton Topological Insulator. *Nature* **2018**, *562*, 552–556.
- [24] Mukamel, S.; Deng, Z.; Grad, J. Dielectric Response, Nonlinear-Optical Processes, and the Bloch-Maxwell Equations for Polarizable Fluids. *J. Opt. Soc. Am. B* **1988**, *5*, 804–816.
- [25] Fontanesi, L.; Mazza, L.; Rocca, G. C. L. Organic-Based Microcavities with Vibronic Progressions: Linear Spectroscopy. *Phys. Rev. B* **2009**, *80*, 235313.
- [26] Toyozawa, Y. On the Dynamical Behavior of an Exciton. *Progr. Theor. Phys. Suppl.* **1959**, *12*, 111–140.
- [27] Mazza, L.; Fontanesi, L.; Rocca, G. C. L. Organic-Based Microcavities with Vibronic Progressions: Photoluminescence. *Phys. Rev. B* **2009**, *80*, 235314.

- [28] Fainberg, B. D. Mean-Field Electron-Vibrational Theory of Collective Effects in Photonic Organic Materials. Long-Range Frenkel Exciton Polaritons in Nanofibers of Organic Dye. *AIP Advances* **2018**, *8*, 075314.
- [29] Eisfeld, A.; Briggs, J. S. Absorption Spectra of Quantum Aggregates Interacting via Long-Range Forces. *Phys. Rev. Lett.* **2006**, *96*, 113003.
- [30] Stepanov, B. I. Universal Relation Between Absorption and Luminescence Spectra of Complex Molecules. *Dokl. Akad. Nauk SSSR* **1957**, *112*, 839–841.
- [31] Davydov, A. S. *Theory of Molecular Excitons*; Plenum: New York, 1971.
- [32] Mukamel, S. *Principles of Nonlinear Optical Spectroscopy*; Oxford University Press: New York, 1995.
- [33] Fainberg, B. D. Ultrafast Dynamics and Non-Markovian Processes in Four-Photon Spectroscopy. In *Advances in Multiphoton Processes and Spectroscopy*, Vol. 15; Lin, S. H.; Vilaey, A. A.; Fujimura, Y., Eds.; World Scientific: Singapore, New Jersey, London, 2003.
- [34] Fainberg, B. D. Theory of the Non-Stationary Spectroscopy of Ultrafast Vibronic Relaxations in Molecular Systems on the Basis of Degenerate Four-Wave Mixing. *Opt. Spectrosc.* **1990**, *68*, 305–309.
- [35] Fainberg, B. Learning About Non-Markovian Effects by Degenerate Four-Wave-Mixing Processes. *Phys. Rev. A* **1993**, *48*, 849–850.
- [36] Fainberg, B. D. Non-Linear Polarization and Spectroscopy of Vibronic Transitions in the Field of Intensive Ultrashort Pulses. *Chem. Phys.* **1990**, *148*, 33–45.
- [37] Fainberg, B. D. Nonperturbative Analytic Approach to Interaction of Intense Ultrashort Chirped Pulses with Molecules in Solution: Picture of "Moving" Potentials. *J. Chem. Phys.* **1998**, *109*, 4523–4532.
- [38] Fainberg, B. D.; Levinsky, B. Stimulated Raman Adiabatic Passage in a Dense Medium. *Adv. Phys. Chem.* **2010**, *2010*, 798419.
- [39] Haug, H.; Koch, S. W. *Quantum Theory of the Optical and Electronic Properties of Semiconductors*; World Scientific: Singapore, 2001.
- [40] Rautian, S. G.; Sobel'man, I. I. The Effect of Collisions on the Doppler Broadening of Spectral Lines. *Soviet Physics Uspekhi* **1967**, *9*, 701–716 [*Usp. Fiz. Nauk* 90, 209-238 (1966)].
- [41] Fainberg, B. D.; Narbaev, V. Chirped Pulse Excitation in Condensed Phase Involving Intramolecular Modes Studied by Double-Sided Feynman Diagrams for Fast Electronic Dephasing. *J. Chem. Phys.* **2000**, *113*, 8113–8124.
- [42] Fainberg, B. D.; Narbaev, V. Chirped Pulse Excitation in Condensed Phase Involving Intramolecular Modes. II. Absorption Spectrum. *J. Chem. Phys.* **2002**, *116*, 4530–4541.
- [43] Abramowitz, M.; Stegun, I. *Handbook on Mathematical Functions*; Dover: New York, 1964.
- [44] Fainberg, B. D. Stochastic Theory of the Spectroscopy of Optical Transitions Based on Four-Photon Resonance Interaction and Photo-Echo-Type Effects. *Opt. Spectrosc.* **1985**, *58*, 323–328.
- [45] Litinskaya, M. Exciton Polariton Kinematic Interaction in Crystalline Organic Microcavities. *Phys. Rev. B* **2008**, *77*, 155325.
- [46] Yee, T. K.; Gustafson, T. K. Diagrammatic Analysis of the Density Operator for Nonlinear Optical Calculations: Pulsed and CW Responses. *Phys. Rev. A* **1978**, *18*, 1597–1617.
- [47] Chovan, J.; Perakis, I. E.; Ceccarelli, S.; Lidzey, D. G. Controlling the Interactions Between Polaritons and Molecular Vibrations in Strongly Coupled Organic Semiconductor Microcavities. *Phys. Rev. B* **2008**, *78*, 045320.

- [48] Schwartz, T.; Hutchison, J. A.; Leonard, J.; Genet, C.; Haacke, S.; Ebbesen, T. W. Polariton Dynamics under Strong Light-Molecule Coupling. *ChemPhysChem* **2013**, *14*, 125–131.
- [49] Litinskaya, M.; Reineker, P.; Agranovich, V. M. Exciton-Polaritons in Organic Microcavities. *Journal of Luminescence* **2006**, *119–120*, 277–282.
- [50] Halas, N. J.; Lal, S.; Chang, W.-S.; Link, S.; Nordlander, P. Quantum Plexcitonics: Strongly Interacting Plasmons and Excitons. *Chem. Rev.* **2011**, *111*, 3913–3961.
- [51] White, A. J.; Fainberg, B. D.; Galperin, M. Collective Plasmon-Molecule Excitations in Nanjunctions: Quantum Consideration. *J. Phys. Chem. Lett.* **2012**, *3*, 2738–2743.
- [52] Sukharev, M.; Nitzan, A. Optics of Exciton-Plasmon Nanomaterials. *J. Phys.: Condens. Matter* **2017**, *29*, 443003.
- [53] Sukharev, M.; Charron, E. Molecular Plasmonics: The Role of Rovibrational Molecular States in Exciton-Plasmon Materials under Strong-Coupling Conditions. *Phys. Rev. B* **2017**, *95*, 115406.
- [54] Fain, V. M.; Khanin, Y. I. *Quantum Electronics*; volume 1. Basic Theory Pergamon Press: Braunschweig, 1969.
- [55] Lin, S. H. Spectral Band Shape of Absorption and Emission of Molecules in Dense Media. *Theor. Chim. Acta* **1968**, *10*, 301–310.

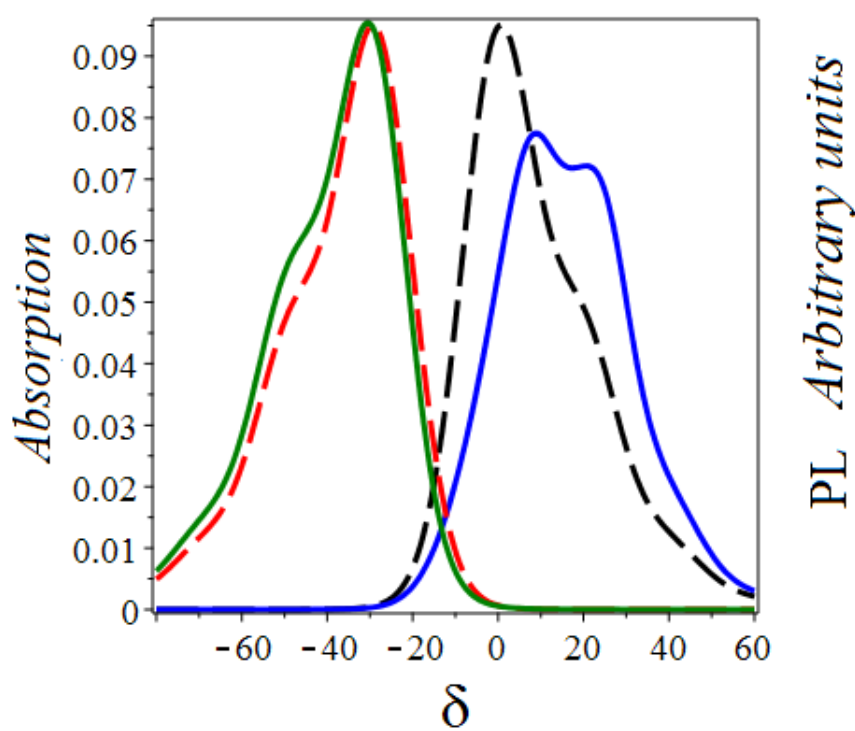
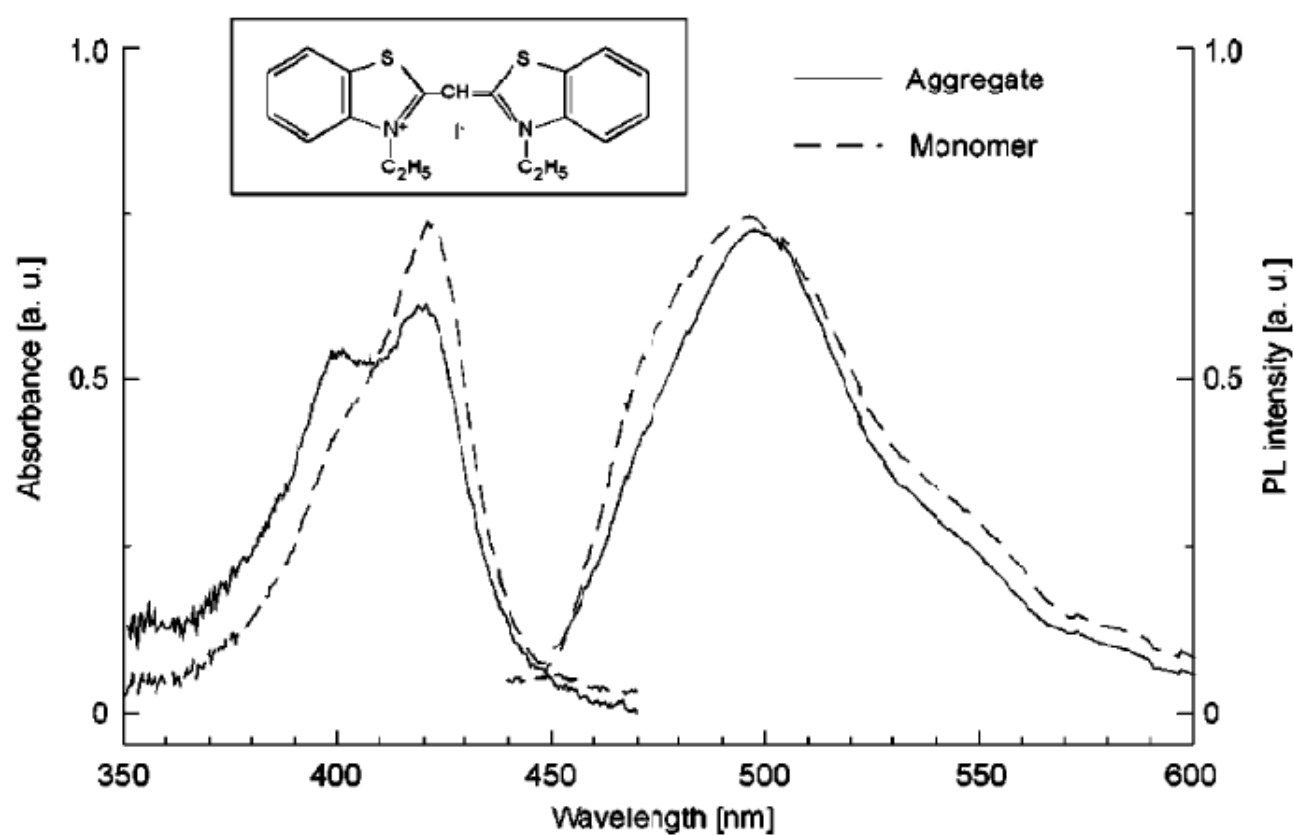


Figure 5.

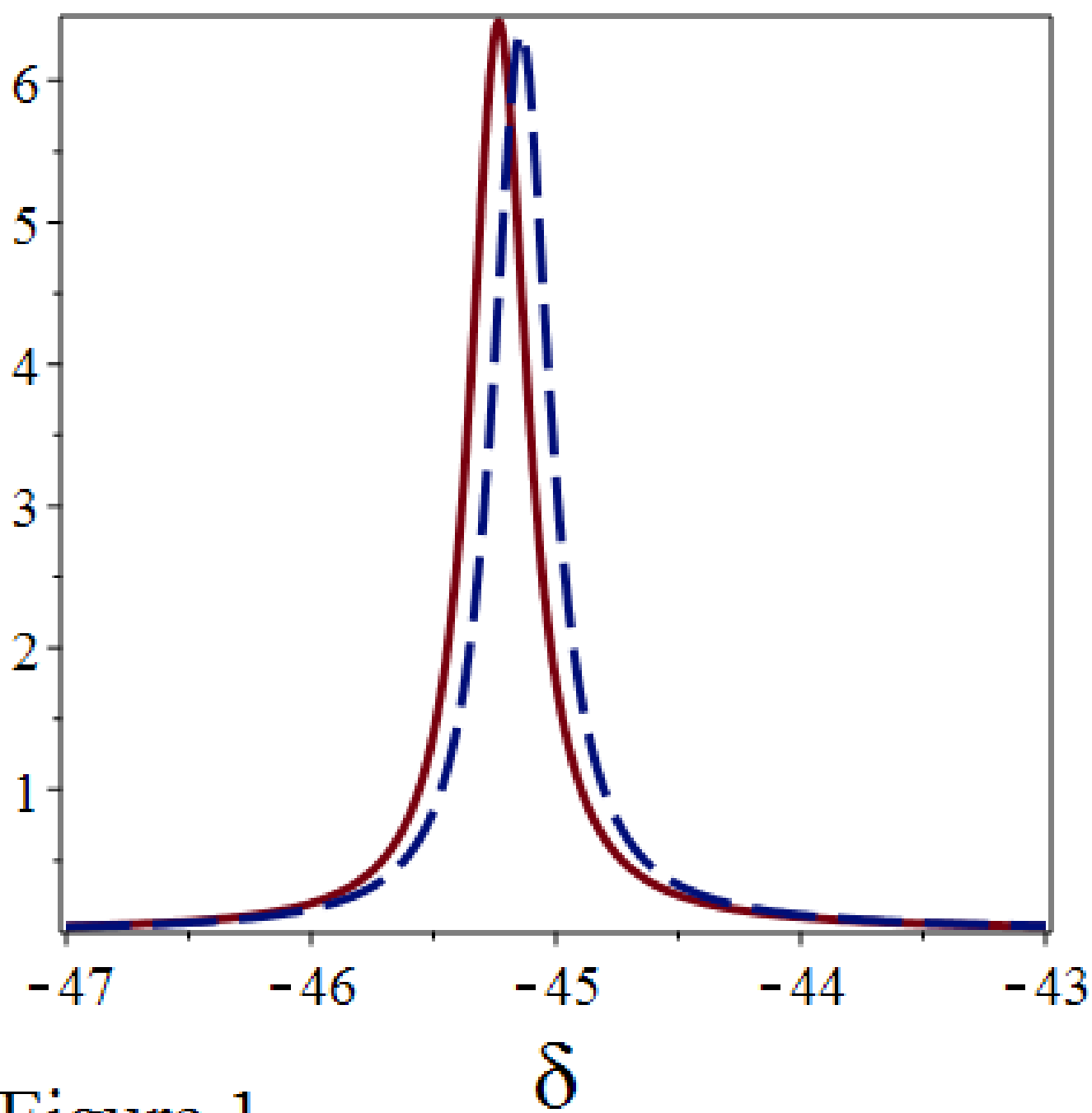


Figure 1

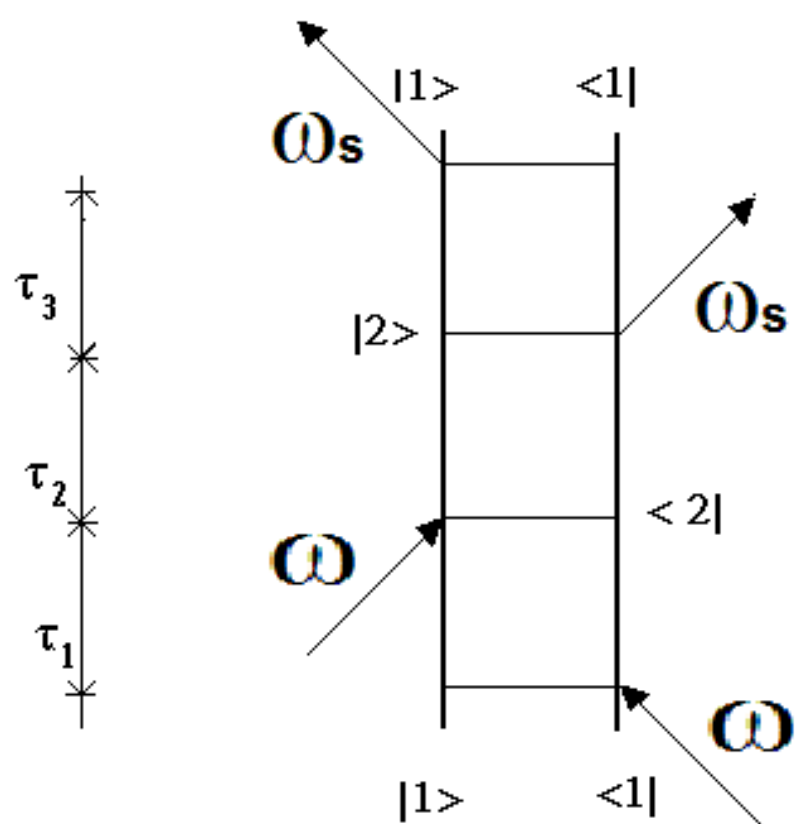
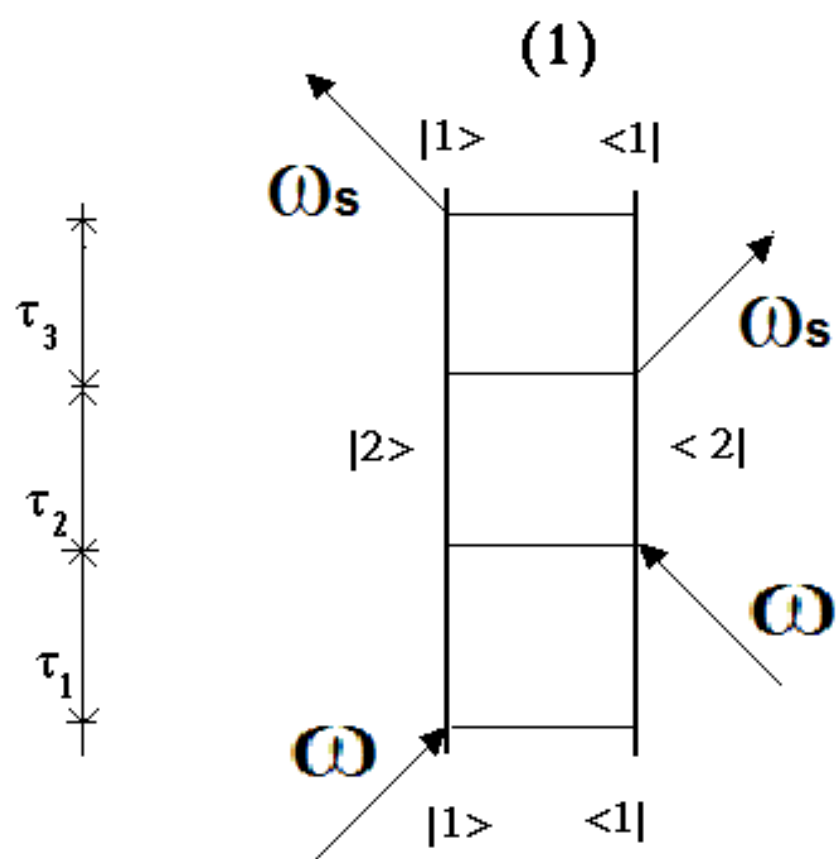


Figure 2.

(2)

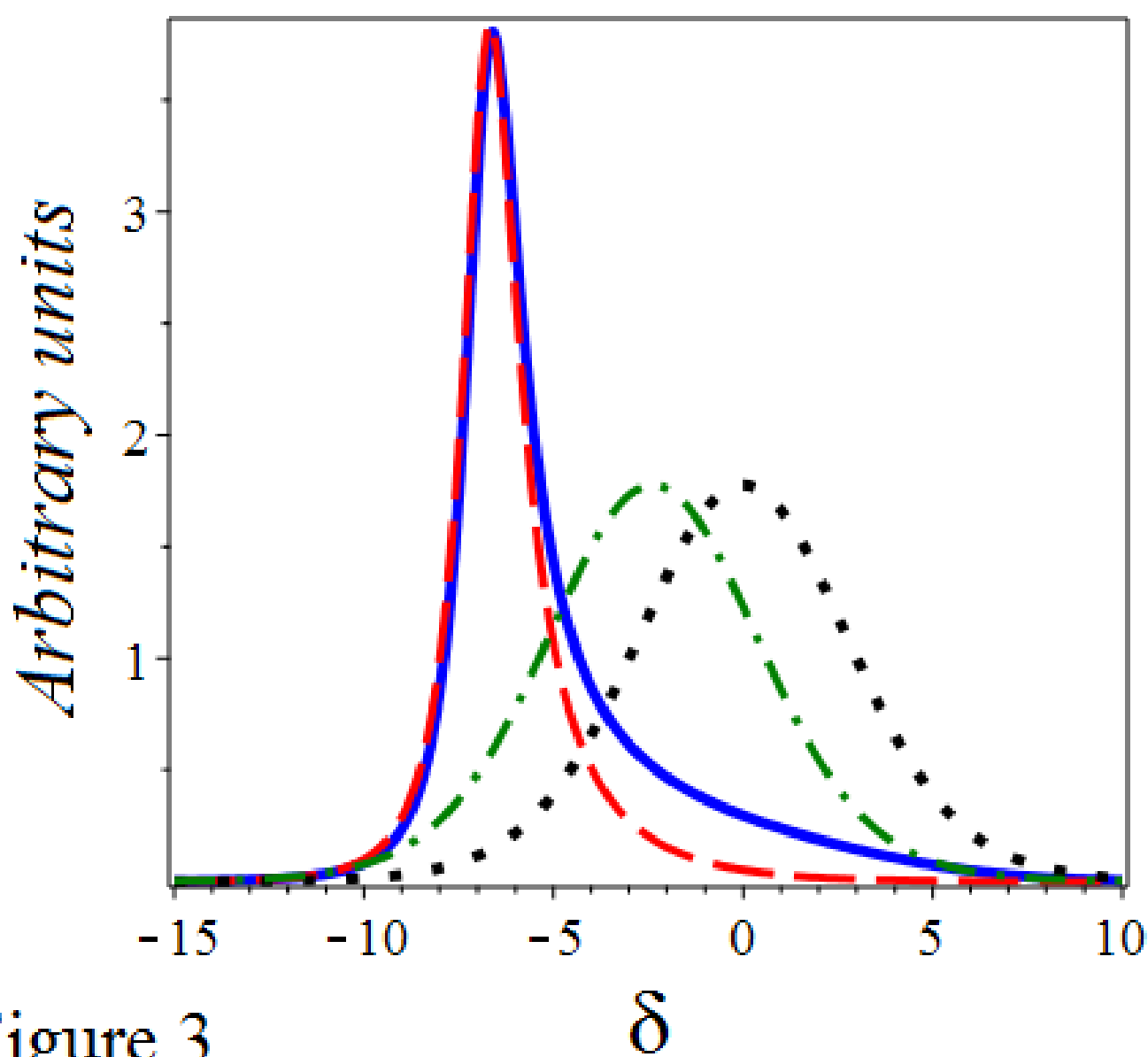
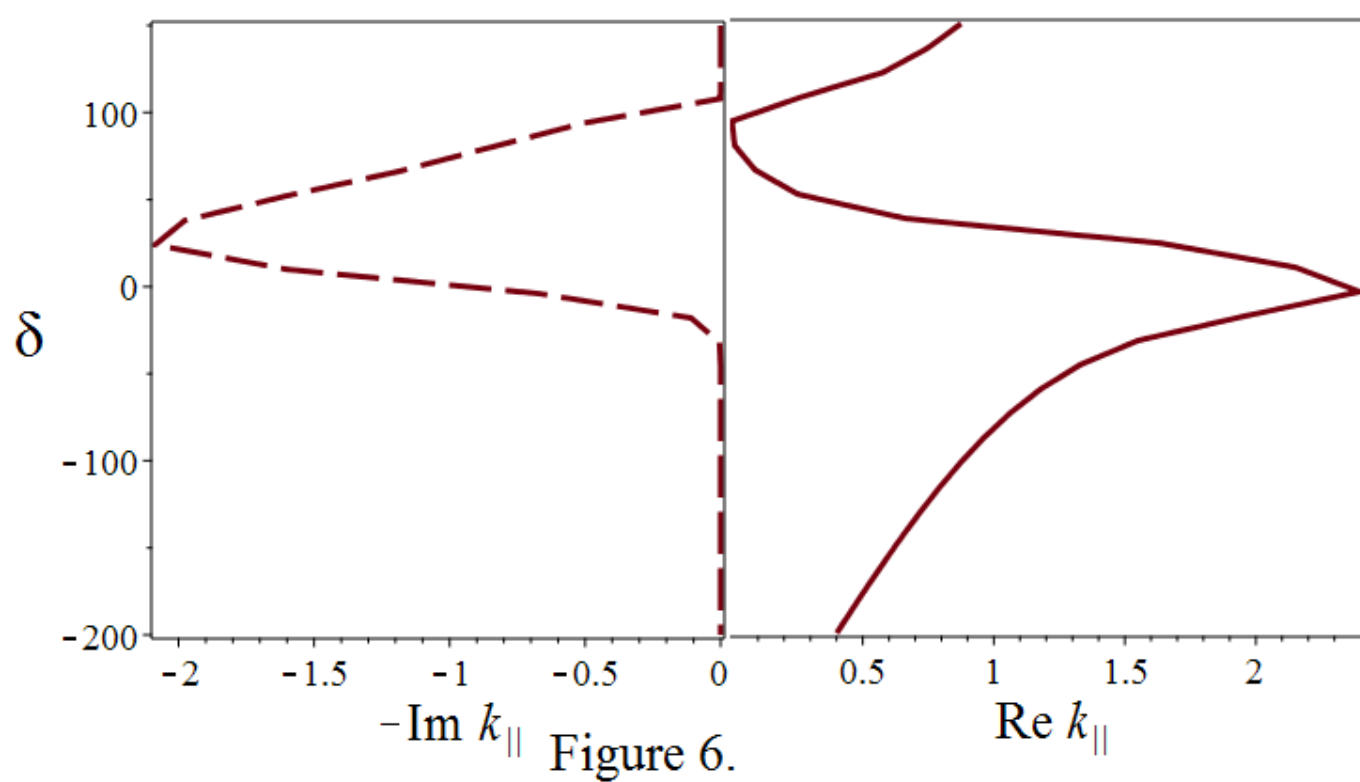


Figure 3.



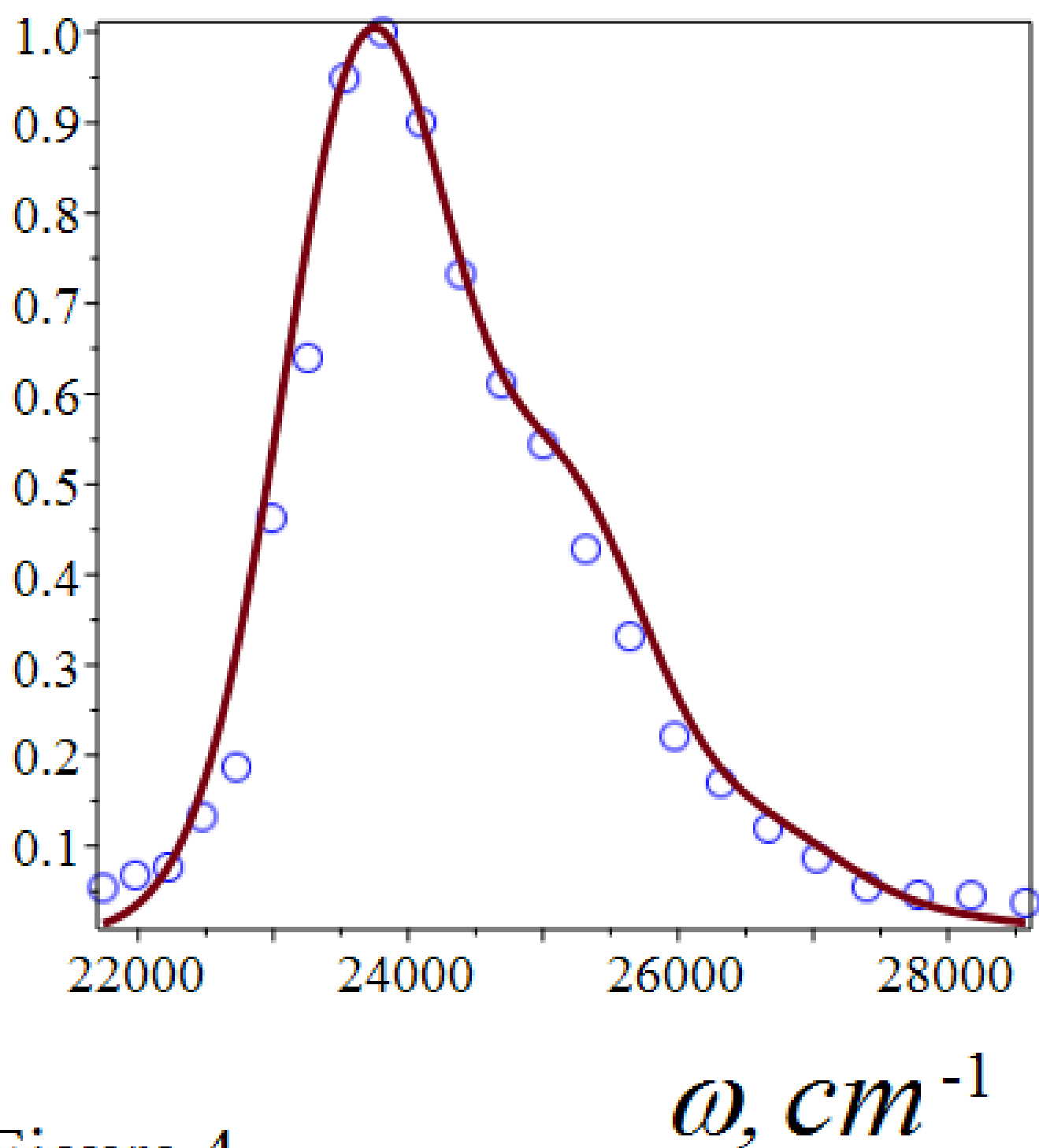


Figure 4.

